Podoplanin negatively regulates CD4+ effector T cell responses

Anneli Peters,[1] Patrick R. Burkett,[1,2] Raymond A. Sobel,[3] Christopher D. Buckley,[4] Steve P. Watson,[5] Estelle Bettelli,[6] and Vijay K. Kuchroo[1]

[1]Evergrande Center for Immunologic Diseases, Harvard Medical School and Brigham and Women's Hospital, Boston, Massachusetts, USA. [2]Pulmonary and Critical Care Division, Department of Medicine, Brigham and Women's Hospital, Boston, Massachusetts, USA. [3]Palo Alto Veteran's Administration Health Care System and Department of Pathology, Stanford University School of Medicine, Stanford, California, USA. [4]Rheumatology Research Group, Center for Translational Inflammation Research, Queen Elizabeth Hospital, Birmingham, United Kingdom. [5]Center for Cardiovascular Sciences, Institute for Biomedical Research, College of Medical and Dental Sciences, University of Birmingham, Birmingham, United Kingdom. [6]Benaroya Research Institute, Seattle, Washington, USA.

Podoplanin (PDPN, also known as Gp38) is highly expressed on the surface of lymphatic endothelial cells, where it regulates development of lymphatic vessels. We have recently observed that PDPN is also expressed on effector T cells that infiltrate target tissues during autoimmune inflammation; however, the function of PDPN in T cells is largely unclear. Here, we demonstrated that global deletion of *Pdpn* results in exaggerated T cell responses and spontaneous experimental autoimmune encephalomyelitis (EAE) in mice with a susceptible genetic background. In contrast, T cell–specific overexpression of PDPN resulted in profound defects in IL-7–mediated T cell expansion and survival. Consequently, these animals exhibited a more rapid resolution of CNS inflammation, characterized by a reduced effector CD4+ T cell population in the CNS. Mice harboring a T cell–specific deletion of *Pdpn* developed exacerbated EAE, with increased accumulation of effector CD4+ T cells in the CNS. Transcriptional profiling of naturally occurring PDPN+ effector T cells in the CNS revealed increased expression of other inhibitory receptors, such as *Pd1* and *Tim3*, and decreased expression of prosurvival factors, including *Il7ra*. Together, our data suggest that PDPN functions as an inhibitory molecule on T cells, thereby promoting tissue tolerance by limiting long-term survival and maintenance of CD4+ effector T cells in target organs.

Introduction

Many autoimmune diseases, including multiple sclerosis (MS), are driven by self-reactive T helper cells that promote autoimmune tissue inflammation, particularly after differentiation into Th1 or Th17 subsets (1). In order to maintain peripheral and tissue tolerance, self-reactive T effector cells that escape negative selection in the thymus are actively controlled in the periphery by a number of mechanisms, including expression of inhibitory cell surface receptors. Cytotoxic T-lymphocyte antigen-4 (CTLA-4), programmed death-1 (PD-1), T cell immunoreceptor with immunoglobulin and ITIM domains (TIGIT), and T cell immunoglobulin- and mucin domain–containing molecule 3 (TIM-3) (2) are essential for controlling autoreactive T cells, as loss of these inhibitory receptors results in hyperproliferation of effector T cells, induction of spontaneous inflammation, and severe autoimmunity. Consistent with this, the *CTLA4* and *PD1* genes have been identified as MS susceptibility loci (2), as defects in or dysregulation of inhibitory pathways allow self-reactive T cell responses to go unabated.

Therapeutic approaches using the inhibitory effects of these receptors are under active investigation and have already yielded remarkable results in the field of cancer immunotherapy, in which blockade of inhibitory pathways significantly improved antitumor T cell responses (3). Interestingly, combined blockade of TIM-3 and PD-1 in mouse tumor models appears to be even more potent in promoting antitumor immune responses (4), suggesting that targeting multiple inhibitory receptors may provide therapeutic synergy. Analogously, dampening self-reactive T cell responses in autoimmunity by modulation of inhibitory receptor function represents an exciting area for therapeutic development. Thus, the identification of additional inhibitory molecules may be of great value. In particular, since autoreactive Th17 cells cause severe inflammation and irreversible tissue damage, molecules that preferentially modulate Th17 cell function are especially promising targets for controlling tissue injury in autoimmune disease.

Using gene expression profiling, we discovered that podoplanin (PDPN), a 43-kDa transmembrane sialomucin-like glycoprotein, is preferentially expressed on the surface of in vitro–differentiated Th17 cells but not on other effector T cell subsets (5). Moreover, during the development of experimental autoimmune encephalomyelitis (EAE) in vivo, PDPN is expressed on the surface of Th17 cells that infiltrate the target tissue. We further showed that blockade of PDPN inhibits formation of ectopic lymphoid follicles (eLFs) in the CNS induced by adoptive transfer of myelin oligodendrocyte glycoprotein–specific (MOG-specific) Th17 cells (5). However, because PDPN is also expressed on many other cell types, including lymphatic endothelial cells, fibroblastic reticular cells, follicular dendritic cells, and subsets of macrophages (6, 7), the functional role of PDPN specifically on T cells has not been elucidated.

Authorship note: Anneli Peters and Patrick R. Burkett contributed equally to this work.
Conflict of interest: Vijay K. Kuchroo is a founder of, and has a financial interest in, Tempero Pharmaceuticals.
Submitted: December 9, 2013; **Accepted:** October 23, 2014.
Reference information: *J Clin Invest*. 2015;125(1):129–140. doi:10.1172/JCI74685.

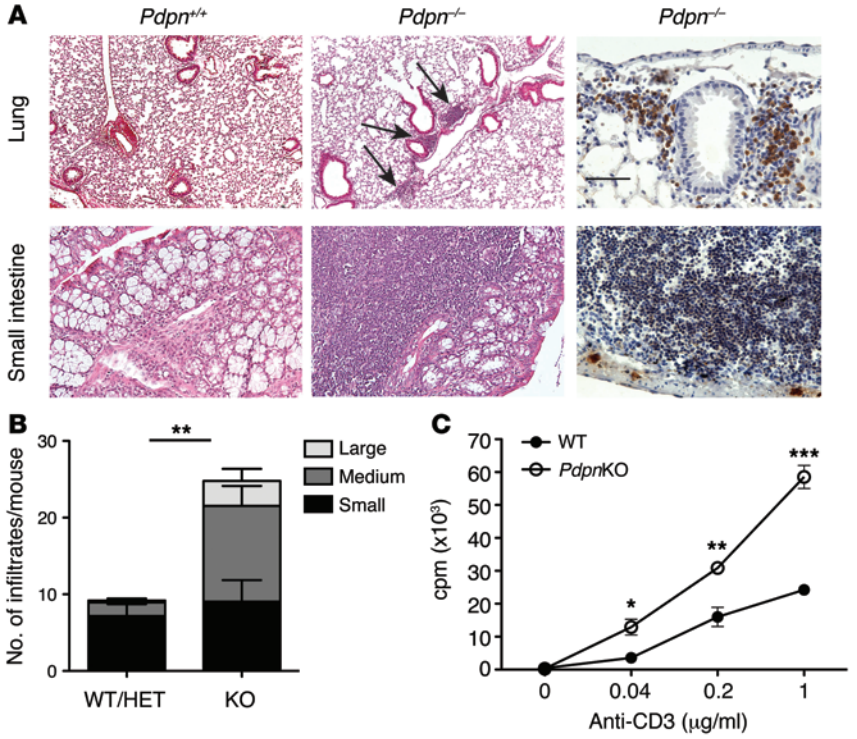

Figure 1. PDPN-deficient mice show exaggerated T cell responses. (**A**) Lungs and intestines were harvested from PDPN-deficient mice and their WT littermates. Sections of the formalin-fixed and paraffin-embedded tissues were stained with hematoxylin and eosin. Both *Pdpn*$^{-/-}$ lung and small intestine show lymphocytic infiltrates (dark blue, arrows). Sections of lung and intestine were also analyzed for the presence of T cells (CD3, dark brown) by immunohistochemistry (right panels). Scale bar: 50 μm. For more information refer to Supplemental Table 1. (**B**) The number of small, medium, and large infiltrates in the small intestines of PDPN-deficient mice (n = 4) and their WT or heterozygous littermates (n = 4) was quantified. (**C**) Sorted naive T cells from PDPN-deficient mice and their WT littermates were stimulated in vitro with different concentrations of anti-CD3 in the presence of irradiated APCs for 72 hours. Proliferation was measured by thymidine incorporation in the last 18 hours. Data shown are representative of 3 or more independent experiments. $^{*}P < 0.05$, $^{**}P < 0.01$, $^{***}P < 0.001$.

To further investigate the role and function of PDPN on CD4 T cells during CNS inflammation, we have analyzed the effects of both loss and overexpression of PDPN on T cell responses using global PDPN-deficient mice, T cell–specific *Pdpn* transgenic mice, and T cell–specific PDPN-deficient mice. Our results demonstrate that PDPN acts as an inhibitory molecule on T cells by limiting survival and maintenance of CD4 effector T cells in target tissues. As PDPN is primarily expressed on T cells infiltrating such tissues, our results suggest that one important function of PDPN on T cells is to inhibit their survival in the target tissues and thus promote tissue tolerance.

Results

PDPN-deficient mice have enhanced T cell responses. To study the role of PDPN in T cell biology, we characterized the T cell phenotype of PDPN-deficient mice. Although *Pdpn*$^{-/-}$ mice on the 129Sv genetic background suffer from defects in heart and lung development and die shortly after birth due to respiratory failure (8, 9), we previously described that PDPN-deficient mice can survive on a mixed 129Sv × C57BL/6 background and reach adulthood, albeit with very low frequency (5). In the few surviving mice, we consistently observed exaggerated immune responses. As we have shown previously, PDPN-deficient mice have a defect in forming normally structured peripheral lymph nodes and thus do not develop lymphadenopathy. However, PDPN-deficient mice consistently developed moderate splenomegaly, while thymic cell numbers were normal (Supplemental Figure 1; supplemental material available online with this article; doi:10.1172/JCI74685DS1). Along with splenomegaly, we also found increased lymphocytic infiltrates in several organs in PDPN-deficient mice when compared with *Pdpn*$^{+/-}$ or *Pdpn*$^{+/+}$ littermates. Affected organs included lung, liver, and large and small intestine, whereas heart and CNS were spared (Figure 1A and Supplemental Table 1). A more detailed histological analysis of the intestine showed that the number of infiltrates, in particular those of medium and large size, was significantly increased in PDPN-deficient mice (Figure 1, A and B). The phenotype of *Pdpn*$^{-/-}$ mice thus bears resemblance to what has been observed in mice lacking molecules that inhibit T cell responses, such as CTLA-4– or PD-1–deficient mice (10, 11), and prompted us to further characterize the cells spontaneously infiltrating the lungs and livers of *Pdpn*$^{-/-}$ mice. As expected, the total number of cells isolated from lungs and livers was significantly higher in PDPN-deficient mice compared with that in *Pdpn*$^{+/-}$ or *Pdpn*$^{+/+}$ littermates (Supplemental Figure 1). The cellular composition of the infiltrates in lungs and livers of PDPN-deficient mice was highly variable, as they contained differing frequencies of B cells, macrophages, and dendritic cells. However, we consistently detected substantial T cell infiltration in organs from PDPN-deficient mice by immunohistochemistry (Figure 1A). To analyze the effect of PDPN deficiency more specifically on T cells, we sorted naive T cells (CD4^{+}CD62L^{hi}) from *Pdpn* knockout (*Pdpn*KO) mice and their WT littermates and measured expansion in response to anti-CD3. Importantly, *Pdpn*KO T cells expanded significantly more than WT T cells, suggesting that lack of PDPN promotes a hyperproliferative T cell phenotype (Figure 1C).

Next, we crossed PDPN-deficient mice to 2D2 mice, which bear a transgenic T cell receptor specific for MOG (12). Importantly, all 2D2 *Pdpn*$^{-/-}$ mice developed spontaneous EAE at around the age of 6 weeks, with a mean maximum score of 2.6 ± 0.2, whereas the 2D2 *Pdpn*$^{+/-}$ littermates remained free of clinical signs of disease (Table 1). Consistent with the clinical data, histological analysis of the CNS showed that 2D2 *Pdpn*$^{-/-}$ mice had demyelination and inflammatory lesions in meninges and parenchyma, whereas no lesions were found in the CNS of 2D2 *Pdpn*$^{+/-}$ littermates (Table 1).

Table 1. 2D2 *Pdpn*KO mice develop spontaneous EAE

Mice	Incidence of EAE	Age at onset (wk)	Mean max. score	No. of meningeal lesions	No. of parenchymal lesions	No. of total lesions
2D2 *Pdpn*$^{+/-}$	0/6	N/A	N/A	1 ± 1	0 ± 0	1 ± 1
2D2 *Pdpn*$^{-/-}$	4/4	6.4 ± 0.2	2.6 ± 0.3	82 ± 7	85 ± 20	167 ± 21

max., maximum; N/A, nonapplicable.

These data further indicate that global lack of PDPN leads to a hyperactive T cell phenotype in vivo and spontaneous T cell–mediated autoimmune disease on a susceptible background.

Overexpression of PDPN causes severe peripheral T cell lymphopenia. Based on our observations, the spontaneous exaggerated T cell responses in PDPN-deficient mice may be due to the lack of PDPN on T cells themselves. However, aside from T cells, PDPN is also expressed on other cell types, including, for example, subsets of macrophages, follicular dendritic cells, fibroblastic reticular cells, and lymphatic endothelial cells. Thus, the analysis and interpretation of data from globally PDPN-deficient mice is complicated by the fact that lack of PDPN on other cell types may also modulate T cell responses. Moreover, the extremely poor survival of PDPN-deficient mice combined with their mixed genetic background resulted in high experimental variability and made a more detailed analysis of the T cell phenotype of globally PDPN-deficient mice unfeasible.

To overcome these hurdles and to study the role of PDPN in T cell biology more specifically, we generated T cell–specific *Pdpn* transgenic mice that express *Pdpn* under the control of the human *CD2* promoter (referred to herein as *Pdpn*TG mice [also known as Tg(*Cd2-Pdpn*) mice]) (Supplemental Figure 2). We obtained 3 different *Pdpn*TG founder lines with different levels of *Pdpn* expression. All 3 lines were viable and fertile, had normal life expectancies, and did not show any obvious developmental abnormalities. Importantly, we saw no evidence of increased PDPN expression in CD19$^+$ B cells or CD11b/CD11c$^+$ myeloid cells isolated from the secondary lymphoid organs of *Pdpn*TG mice (Supplemental Figure 3A). Additionally, overexpression of PDPN in the T cell compartment did not alter the relative frequency of lymph node stromal cell populations (Supplemental Figure 3B), supporting that selective overexpression only occurs in T cells. Analysis of PDPN expression levels on peripheral T cells revealed that founder line 552 was a low expressor, i.e., 5%–10% of the CD4 T cells and 3%–8% of the CD8 T cells isolated from lymph nodes or spleens expressed PDPN (Figure 2A and Supplemental Figure 3, C and D). In contrast, founder line 560 was a high expressor, with the majority (50%–80%) of peripheral CD4 T cells expressing PDPN. The fraction of PDPN-positive CD8 T cells in the high expressor lines was

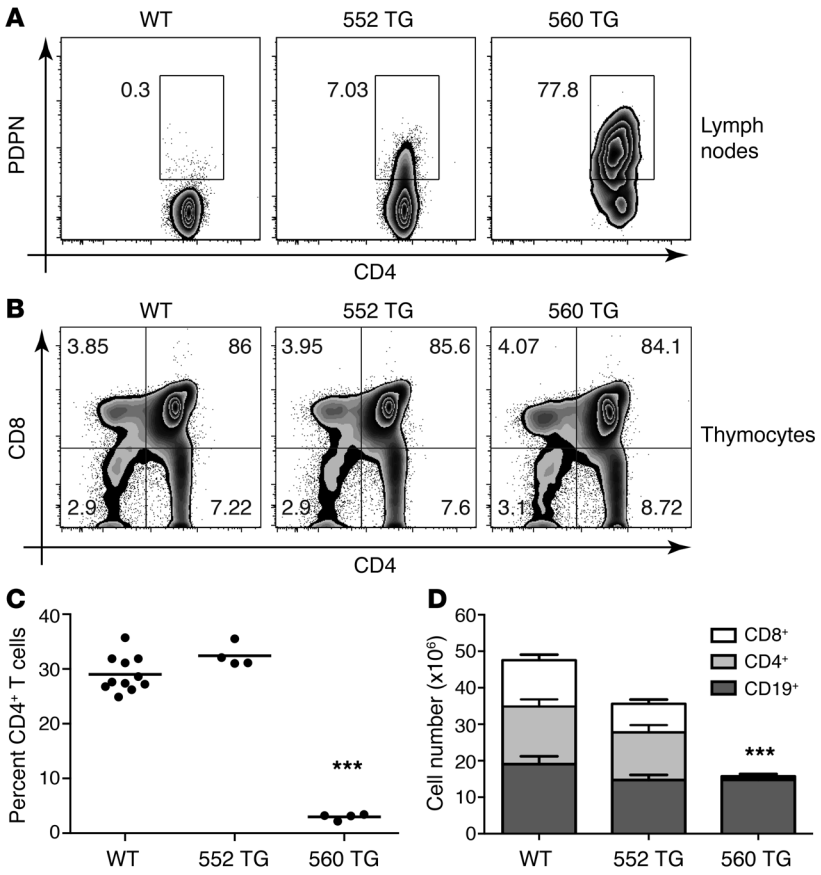

Figure 2. PDPN T cell transgenic mice develop severe peripheral lymphopenia. (**A**) Lymph nodes were harvested from 2 independent lines of 6- to 12-week-old *Pdpn*TG mice and their WT littermates. CD4 T cells were analyzed for expression of PDPN by flow cytometry. Numbers represent the percentage of CD4 T cells. (**B**) Thymuses were harvested from 2 independent lines of 6- to 12-week-old *Pdpn*TG mice and their WT littermates and analyzed for the presence of CD8$^+$ and CD4$^+$ T cell populations by flow cytometry. Numbers represent the percentage of total thymocytes. Data are representative of >5 mice of each group. (**C**) Total lymph node cells from 2 lines of *Pdpn*TG mice and their WT littermates were analyzed for the presence and percentage of CD4 T cells. Data points represent individual mice (n = 4 or more). Horizontal bars indicate the mean. (**D**) The total number of CD8 and CD4 T cells as well as CD19 B cells in the spleens of 2 lines of *Pdpn*TG mice and their WT littermates was determined by flow cytometry. All data are representative of at least 3 independent experiments. ***P < 0.001.

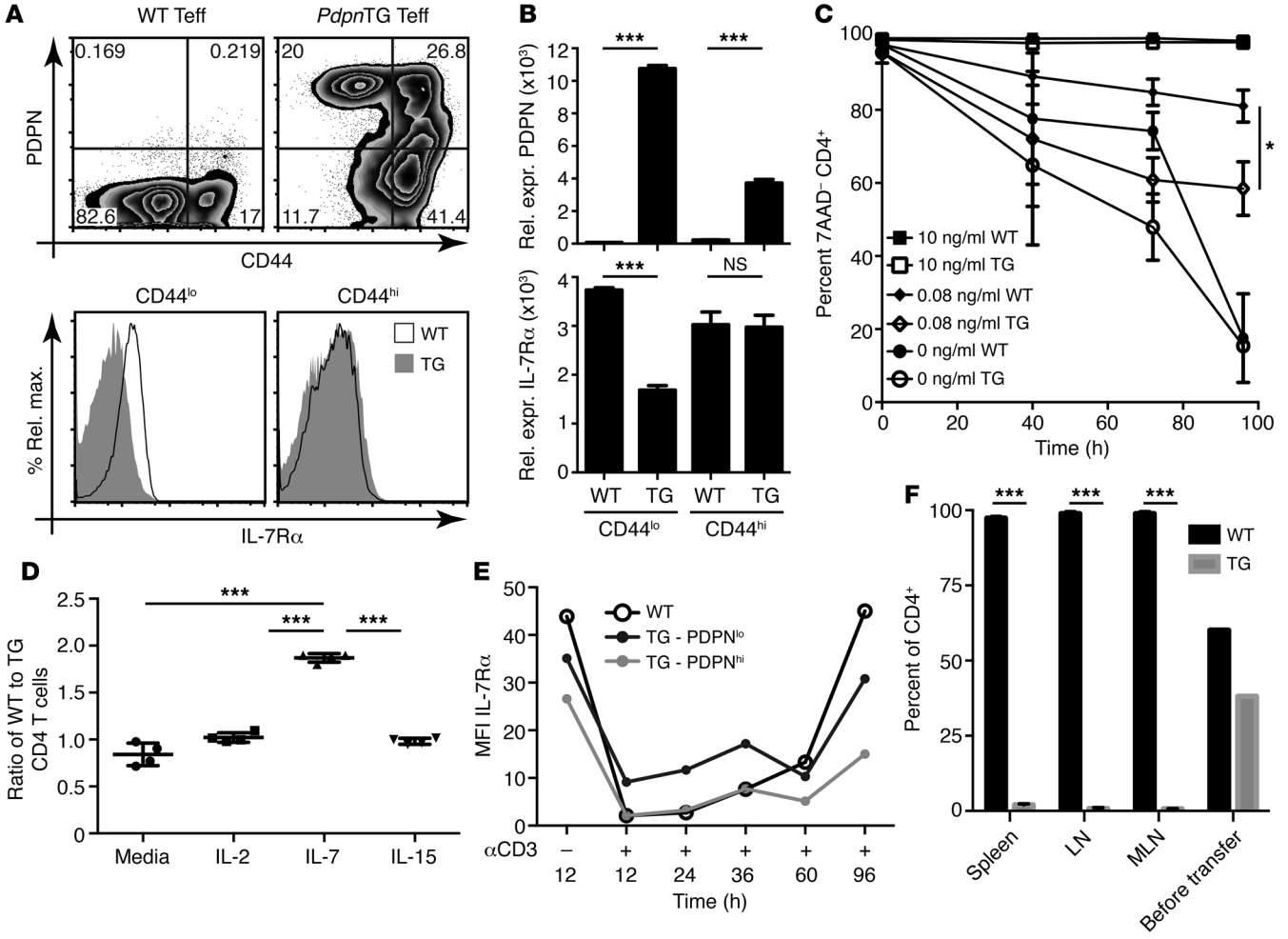

Figure 3. Overexpression of PDPN limits IL-7–dependent T cell survival. (**A**) Splenocytes from WT and *Pdpn*TG mice (line 560) were analyzed for expression of CD44, PDPN, and IL-7Rα on CD4⁺FOXP3/GFP⁻ T effector cells (Teff) by flow cytometry. Numbers represent the percentage of CD4 T cells. (**B**) RNA was isolated from CD4⁺Foxp3.GFP⁻CD44^{hi} and CD4⁺Foxp3.GFP⁻CD44^{lo} T cells sorted from spleens and lymph nodes of naive WT and *Pdpn*TG mice (line 560). Expression of PDPN and IL-7Rα was assessed by quantitative PCR. (**C**, **D**, and **F**) CD4 T cells were purified from Ly5.1 WT and Ly5.2 *Pdpn*TG mice (line 560) and mixed. (**C**) Cells were cultured in vitro with the indicated concentrations of IL-7, and the percentage of 7AAD⁻ cells at different time points was determined by flow cytometry. (**D**) Cells were cultured in vitro in the presence of IL-2 (1 ng/ml), IL-7 (1 ng/ml), or IL-15 (10 ng/ml). The ratio of surviving Ly5.1⁺ WT to Ly5.2⁺ *Pdpn*TG CD4 T cells after 96 hours was determined by flow cytometry. Data points represent independent replicates. (**E**) CD4⁺CD25⁻ T cells sorted from WT and *Pdpn*TG mice (line 560) were cultured in vitro in the presence or absence of anti-CD3. The expression of IL-7Rα on T cells was determined by flow cytometry at the indicated time points. (**F**) Mixed Ly5.1⁺ WT and Ly5.2⁺ *Pdpn*TG (line 560) CD4 T cells were adoptively transferred into CD90.1⁺ recipients. Twenty-one days after transfer, the frequency of Ly5.1⁺ WT and Ly5.2⁺*Pdpn*TG cells among CD90.2⁺CD4⁺ cells was determined in the indicated organs. Data shown are representative of at least 2 independent experiments. $^*P < 0.05$, $^{***}P < 0.0001$.

much smaller and more variable (2%–20% in line 560)(Figure 2A and Supplemental Figure 3, C and D). The third founder line (line 556) largely recapitulated the phenotype of the high expressor line 560 and therefore was not included here.

To assess whether overexpression of PDPN affects T cell development, we analyzed the different T cell populations in the thymus. We found normal frequencies and total numbers of double-positive, CD4 single-positive, CD8 single-positive, and double-negative thymocytes in all *Pdpn*TG lines (Figure 2B and Supplemental Figure 4). These data suggest that thymic T cell development is unperturbed in *Pdpn*TG mice.

We next analyzed T cell populations in the spleens and lymph nodes of the transgenic mice. Importantly, we found that frequency and total number of both CD4 and CD8 T cells were almost 10-fold reduced in the high expressor line, whereas the low expressor line had similar frequency and numbers of T cells as WT mice (Figure 2, C and D, and Supplemental Figure 5A). We observed similar degrees of T cell lymphopenia in the high expressor line in spleens and lymph nodes, both in terms of total T cell numbers and percentage of T cells among total live cells. In contrast to CD4 and CD8 T cells, γ/δ T cell numbers were relatively normal in *Pdpn*TG high expressor mice (Supplemental Figure 5B). Similarly, normal numbers of non–T cell populations, including B cells, macrophages, and dendritic cells, were present in spleens and lymph nodes of the *Pdpn*TG high expressor line, although the percentage of B cells and CD11b/c⁺ cells was increased as a consequence of the reduced T cell populations (Figure 2D and Supplemental Figure 5B).

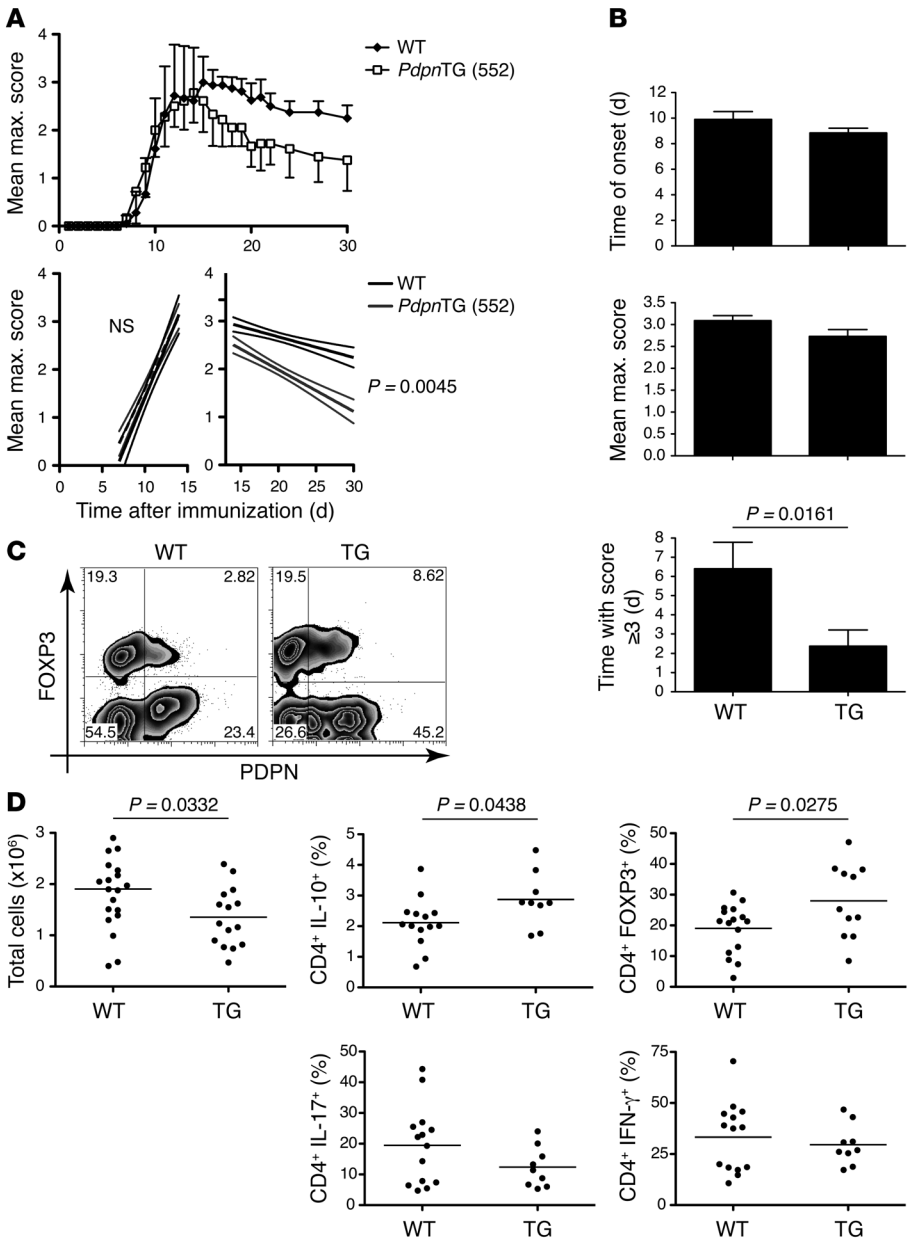

Figure 4. *Pdpn*TG mice recover better from EAE. (**A** and **B**) *Pdpn*TG mice (line 552) and their WT littermates were immunized with MOG/CFA and (**A**) monitored for clinical signs of EAE for 30 days. Linear regression analysis for the onset phase (day 7–14) as well as the recovery phase (day 14–30) of disease is also shown. For the onset phase no significant difference was detected, whereas *Pdpn*TG mice recovered significantly better than WT mice ($P = 0.0045$). Data are representative of at least 4 mice per group and 3 independent experiments. (**B**) Graphs show time of onset, mean maximum score, and time with a score of 3 or higher for WT mice and *Pdpn*TG mice (line 552). For more information also refer to Table 2. (**C**) Mononuclear cells were isolated from the CNS of WT and *Pdpn*TG mice (line 552) at the peak of disease and analyzed for expression of PDPN and FOXP3 by flow cytometry. Plots show live $CD4^+CD11b^-$ T cells only and are representative of more than 3 independent experiments. Numbers represent the percentage of CD4 T cells. (**D**) Mononuclear cells were isolated from the CNS of WT and *Pdpn*TG mice (line 552) at the peak of disease and counted. Cells were analyzed for expression of FOXP3, IL-17A, IFN-γ, and IL-10 by flow cytometry. Data points represent individual mice. Horizontal bars indicate the mean.

Given that only the high expressor *Pdpn*TG mice developed peripheral T cell lymphopenia, while low expressor *Pdpn*TG mice had normal T cell numbers, these data suggest that expression of high levels of PDPN on T cells leads to impaired survival and/or proliferation and interferes with normal T cell homeostasis.

PdpnTG T cells have a defect in IL-7–mediated survival. After exiting the thymus, T cells circulating through peripheral lymphoid organs depend on survival cues for their maintenance and expansion. One of the most important survival signals is provided by the cytokine IL-7, which is mainly produced by the stromal cells of secondary lymphoid organs, and defects in IL-7/IL-7Rα signaling have been shown to cause severe lymphopenia (13). To determine whether the lymphopenia in our *Pdpn*TG high expressor line could be associated with defective IL-7 signaling, we first analyzed $FOXP3^-$ CD4 T effector cells from WT and *Pdpn*TG mice (line 560) for expression of IL-7Rα and PDPN. Interestingly, we found that in *Pdpn*TG mice the naive $CD44^{lo}$ CD4 T cells expressed very high amounts of PDPN but reduced levels of IL-7Rα compared with naive $CD44^{lo}$ CD4 T cells from WT mice. In contrast, memory $CD44^{hi}$ CD4 T cells from *Pdpn*TG mice, which expressed less PDPN than naive *Pdpn*TG CD4 T cells both in terms of percentage and level of expression as determined by MFI, had similar amounts of IL-7Rα compared with memory T cells from WT mice (Figure 3A). Consistent with the protein data, we also found reduced *Il7ra* mRNA levels in naive CD4 effector T cells from *Pdpn*TG mice compared with naive CD4 effector T cells from WT mice, whereas *Il7ra* mRNA levels were comparable between *Pdpn*TG and WT memory T cells (Figure 3B). These data suggest that expression of PDPN and IL-7Rα are inversely correlated in *Pdpn*TG CD4 T cells.

Since PDPN expression was higher and IL-7Rα expression was lower on *Pdpn*TG naive T cells compared with *Pdpn*TG memory T cells, we next determined the frequencies of naive, memory, and

Table 2. EAE in *Pdpn*TG mice (line 552)

Mice	Incidence of EAE	Mortality	Day of onset	Mean max. score	No. of days with score ≥3	No. of meningeal lesions	No. of parenchymal lesions	No. of total lesions
WT	11/14	0/14	9.9 ± 0.6	3.1 ± 0.1	6.4 ± 1.4	73 ± 17	90 ± 19	163 ± 34
*Pdpn*TG	13/15	0/15	8.8 ± 0.3	2.7 ± 0.2	2.4 ± 0.8	15 ± 5	12 ± 5	27 ± 9
P values			NS	NS	$P = 0.0161$	$P = 0.0018$	$P = 0.0002$	$P = 0.0004$

Tregs among the remaining CD4 T cells in *Pdpn*TG mice. Importantly, the frequency of naive T cells was greatly reduced in high expressor *Pdpn*TG mice, whereas frequencies of both activated/memory phenotype T cells and FOXP3$^+$ Tregs were increased (Supplemental Figure 6). Although it is important to note that all T cell populations were reduced in total numbers in high expressor *Pdpn*TG mice (Supplemental Figure 6), these data imply that PDPN overexpression has a greater affect on naive T cells than on activated/memory T cells and Tregs.

We have shown that expression of PDPN and IL-7Rα is inversely correlated in *Pdpn*TG T cells. To test whether *Pdpn*TG CD4 T cells have a defect in IL-7–mediated survival, we cocultured unactivated congenic WT and *Pdpn*TG CD4 T cells (high expressor line 560) in the presence of exogenous IL-7 and monitored their survival. At high concentrations of IL-7, WT and *Pdpn*TG CD4 T cells survived equally well. However, at low concentrations of IL-7, WT CD4 T cells survived much better than *Pdpn*TG CD4 T cells (Figure 3C). We next assessed whether *Pdpn*TG CD4 T cells also demonstrated impaired survival in response to other γ_c-dependent cytokines. While coculture of WT and *Pdpn*TG CD4 T cells with IL-7 resulted in preferential survival of WT CD4 T cells, this was not seen with either IL-2 or IL-15, indicating that *Pdpn*TG CD4 T cells are specifically impaired in their ability to respond to and compete for IL-7 (Figure 3D).

IL-7 signals are essential for slow homeostatic expansion and survival of T cells in the periphery. However, upon antigen encounter and during the ensuing activation phase, CD4 effector T cells rely primarily on TCR stimulation, IL-2, and inflammatory cytokines for proliferation signals rather than IL-7 and thus downregulate expression of IL-7Rα during activation/effector phases of the adaptive immune response. When effector CD4 T cell populations contract after an acute immune response, expression of IL-7Rα is recovered to permit long-term survival of memory-precursor CD4 T cells (14). To determine the kinetics of IL-7Rα expression on *Pdpn*TG T cells during and after activation, we stimulated WT and *Pdpn*TG CD4 T cells with anti-CD3 and followed the expression of IL-7R over time. As expected, 12 hours after activation with anti-CD3, WT CD4 T cells had completely downregulated IL-7Rα compared with cells that were not stimulated with anti-CD3. Over time WT CD4 T cells then slowly regained cell surface expression of IL-7Rα and reached levels comparable to those of unstimulated cells at 96 hours (Figure 3E). In contrast, *Pdpn*TG T cells were not able to recover expression of IL-7Rα nearly as well as WT T cells. Strikingly, among the *Pdpn*TG CD4 T cells, PDPN^{hi} cells had the biggest defect in regaining IL-7Rα expression, whereas PDPN^{lo} cells managed to at least partially restore IL-7Rα expression on the surface, albeit not to WT levels (Figure 3E). These data suggest that PDPN$^+$ CD4 T cells may exhibit impaired survival due to a defect in IL-7Rα expression. To determine whether *Pdpn*TG CD4 T cells also show impaired survival in vivo, CD4 T cells from Ly5.2$^+$Thy1.2$^+$ *Pdpn*TG mice were mixed with Ly5.1$^+$Thy1.2$^+$ WT cells (~60% WT, ~40% transgenic), and adoptively transferred into Thy1.1$^+$ mice. After 3 weeks, over 90% of all transferred Thy1.2$^+$ CD4$^+$ cells in the spleens, lymph nodes, and mesenteric lymph nodes were Ly5.1$^+$ WT cells, while very few Ly5.2$^+$ *Pdpn*TG cells were detected. This experiment demonstrates that overexpression of PDPN in CD4 T cells also impairs their survival in vivo (Figure 3F).

To gain additional insight into the mechanism by which PDPN functions as an inhibitory molecule on T cells, we obtained mice deficient for CLEC-2, a C-type lectin-like receptor that is a binding partner for PDPN (15). Similar to global *Pdpn*$^{-/-}$ mice, global *Clec2*$^{-/-}$ mice on the 129Sv background also exhibit very poor survival rates and have aberrant lymphatic development (16). Upon crossing *Clec2*$^{-/-}$ mice with the high expressor *Pdpn*TG line, we observed an almost complete rescue of the lymphopenic phenotype, as *Clec2*$^{-/-}$ *Pdpn*TG mice had normal numbers of peripheral T cells, whereas their *Clec2*$^{+/-}$ *Pdpn*TG littermates showed severe T cell lymphopenia (Supplemental Figure 7A). In addition, *Clec2*$^{-/-}$ *Pdpn*TG CD4 T cells expressed similar levels of IL-7Rα as *Clec2*$^{-/-}$ CD4 T cells, both in terms of protein and mRNA, while *Clec2*$^{+/-}$ *Pdpn*TG CD4 T cells showed strong downregulation of IL-7Rα compared with *Clec2*$^{+/-}$ controls (Supplemental Figure 7, B and C). These data suggest that the severe T cell lymphopenia and downregulation of IL-7Rα in *Pdpn*TG mice is mediated by a PDPN-CLEC2 interaction.

PdpnTG mice recover better from EAE. We have shown that overexpression of PDPN on CD4 T effector cells impairs their ability to recover expression of IL-7Rα after T cell activation. This supports the hypothesis that, after the acute activation phase of an immune response is over, PDPN$^+$ T cells may not be able to survive due to their impaired ability to respond to IL-7 signals, and thus expression of PDPN on T cells may serve to limit excessive tissue inflammation. To test this hypothesis during CNS inflammation in EAE, we used the low expressor *Pdpn*TG mice (line 552), because these mice have similar numbers of T cells and similar frequencies of naive, memory, and Treg populations at baseline as WT mice. Upon immunization with $MOG_{35–55}$ in CFA for induction of active EAE, WT and low expressor *Pdpn*TG mice developed clinical signs of disease with similar kinetics and reached similar maximum scores, indicating that the acute activation phase of the immune response is comparable between WT and *Pdpn*TG mice (Figure 4, A and B, and Table 2). However, consistent with our hypothesis, *Pdpn*TG mice spent less time at their maximum score (Figure 4B

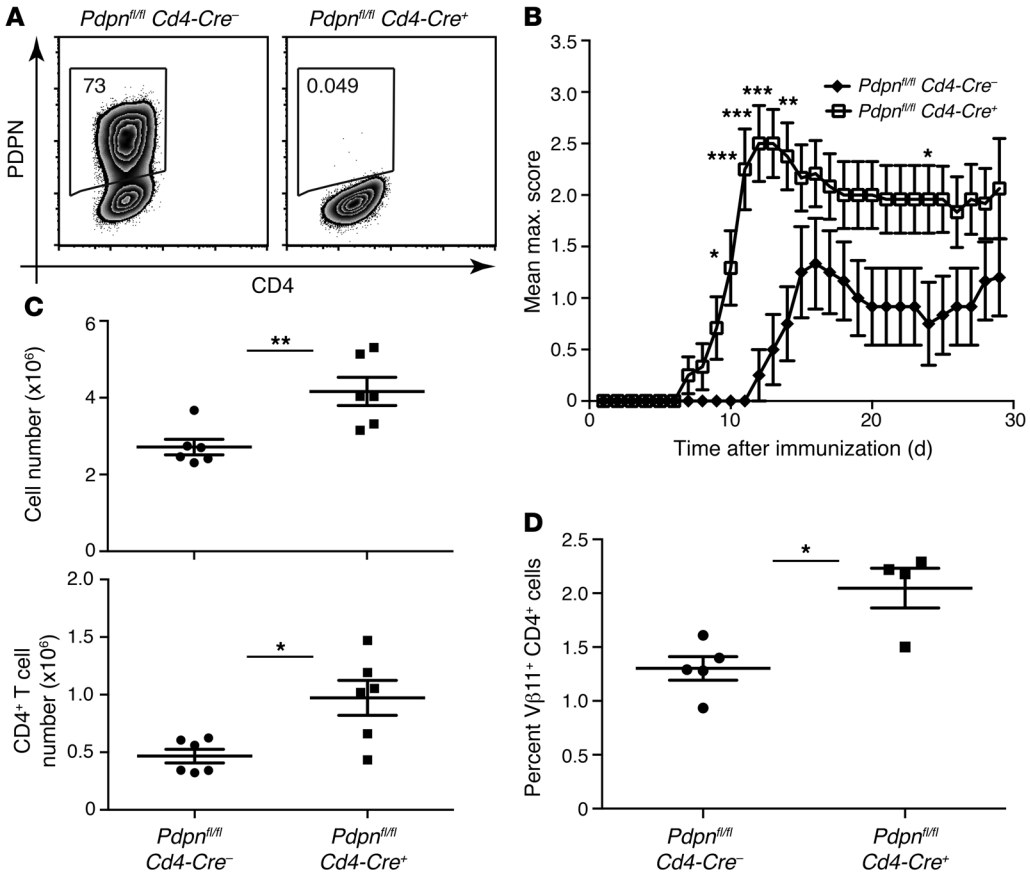

Figure 5. Selective deletion of PDPN in CD4⁺ T cells results in enhanced severity of EAE and increased CD4 T cell accumulation in the CNS. (**A**) CD4 T cells were isolated from *Pdpn*$^{fl/fl}$ *Cd4-Cre*$^{+}$ or *Cd4-Cre*$^{-}$ controls and differentiated into Th17 cells. PDPN expression was assessed by flow cytometry. Data are representative of more than 4 independent experiments. Numbers represent the percentage of CD4 T cells. (**B** and **C**) *Pdpn*$^{fl/fl}$ *Cd4-Cre*$^{+}$ or control *Cd4-Cre*$^{-}$ mice were immunized with MOG/CFA for the development of EAE. (**B**) Average clinical score over 30 days is shown. Data represent pooled data from 2 independent experiments (*Pdpn*$^{fl/fl}$ *Cd4-Cre*$^{+}$, $n = 12$; *Pdpn*$^{fl/fl}$ *Cd4-Cre*$^{-}$, $n = 6$). (**C**) Cells were isolated from the CNS of *Pdpn*$^{fl/fl}$ *Cd4-Cre*$^{+}$ or control mice, and both the total number of infiltrating CD4 T cells as well as the number of infiltrating CD4 T cells was determined. Data points represent individual mice from 2 independent experiments. (**D**) Naive CD4 T cells were isolated from 2D2^{+} *Pdpn*$^{fl/fl}$ *Cd4-Cre*$^{+}$ or 2D2^{+} *Pdpn*$^{fl/fl}$ *Cd4-Cre*$^{-}$ mice and adoptively transferred into WT mice, which were then immunized with MOG/CFA for the development of EAE. Mononuclear cells were isolated from the CNS of mice at day 10 after immunization, and the frequency of transgenic Vβ11^{+}CD4^{+} T cells was determined by flow cytometry. Each data point represents an individual mouse. Data are representative for 2 independent experiments. $^{*}P < 0.05$, $^{**}P < 0.01$, $^{***}P < 0.001$.

and Table 2) and thus recovered better and more quickly than WT mice, as shown by linear regression analysis of the recovery phase (Figure 4A). The improved recovery was also reflected in the histological analysis of the CNS, as we observed fewer lesions in the CNS of *Pdpn*TG mice compared with their WT counterparts (Table 2). To determine the cellular basis of the improved recovery we analyzed the CNS-infiltrating cells. We first analyzed expression of PDPN on CD4 T cells infiltrating the CNS at the peak of disease. Importantly, PDPN expression was consistently higher on both effector and Tregs in the CNS of *Pdpn*TG mice compared with WT mice (Figure 4C), confirming that under acute inflammatory conditions even the low expressor line of *Pdpn*TG mice serves as a good model for PDPN overexpression. Upon isolation of CNS-infiltrating cells at the peak of disease, we found that, despite similar clinical scores, the number of infiltrating cells was already significantly lower in *Pdpn*TG mice compared with that in WT mice (Figure 4D). In addition, the frequencies of IL-10–producing CD4 T cells and FOXP3^{+} Tregs were significantly increased, while the frequencies of IL-17– and IFN-γ–producing CD4 effector T cells were slightly decreased (Figure 4D). These data support the hypothesis that the improved recovery in *Pdpn*TG mice may be due to impaired survival of T effector cells in the CNS: not only did we recover fewer total cells from the CNS of *Pdpn*TG mice, but the frequency of CD4 T effectors was also decreased in favor of an increase in FOXP3^{+} Tregs in *Pdpn*TG mice. Together with an increase of IL-10 producers and a decrease of IL-17/IFN-γ producers, this cellular environment promotes recovery and limits inflammation.

Selective deficiency of PDPN in T cells exacerbates EAE. In order to further investigate the T cell–specific role of PDPN, we used *Pdpn*$^{fl/fl}$ mice crossed to *Cd4-Cre* transgenic mice. Upon in vitro differentiation into Th17 cells, CD4 T cells from *Pdpn*$^{fl/fl}$ *Cd4-Cre* mice expressed no detectable PDPN, unlike cells from control *Pdpn*$^{fl/fl}$ mice, confirming conditional deletion of *Pdpn* (Figure 5A). We next immunized *Pdpn*$^{fl/fl}$ *Cd4-Cre* mice or control *Pdpn*$^{fl/fl}$ mice with $MOG_{35–55}$ in CFA to induce EAE. Notably, *Pdpn*$^{fl/fl}$ *Cd4-Cre* mice developed clinical signs of disease more rapidly and had significantly higher scores between days 10 and 14 ($P < 0.05$) than did control *Pdpn*$^{fl/fl}$ mice (Figure 5B). Consistent with the more rapid onset and increased severity of disease in *Pdpn*$^{fl/fl}$ *Cd4-Cre* mice, we observed increased numbers of CNS-infiltrating cells, including CD4 T cells, in *Pdpn*$^{fl/fl}$ *Cd4-Cre* mice compared with *Cre*-negative controls (Figure 5C). To confirm that PDPN-deficient CD4 T cells preferentially accumulate in the CNS during EAE, we adoptively transferred CD4 T cells isolated from either *Pdpn*$^{fl/fl}$ *Cd4-Cre* or *Pdpn*$^{fl/fl}$ mice expressing the 2D2 TCR transgene into naive mice and then immunized the recipients to induce EAE. We consistently observed a higher frequency of 2D2^{+} T cells (identified by the expression of Vβ11) in the CNS of mice that had received 2D2^{+} *Pdpn*$^{fl/fl}$ *Cd4-Cre* T cells (Figure 5D). Taken together,

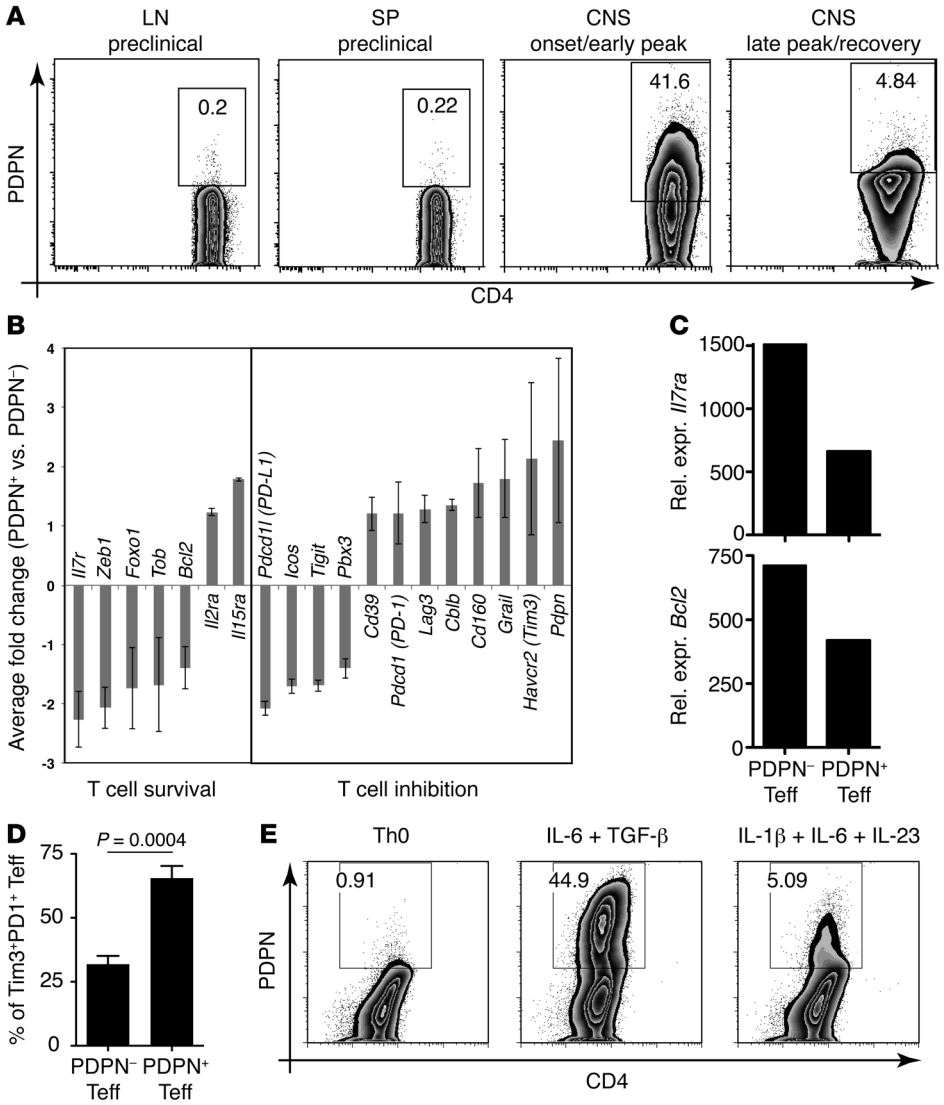

Figure 6. Natural PDPN⁺ T effector cells in the CNS show an inhibited phenotype. (**A**) WT mice were immunized with MOG/CFA for the development of EAE. Expression of PDPN on CD4 T cells isolated from spleens (SP) and lymph nodes 8 days after immunization and from the CNS either at the onset of disease or during recovery was determined by flow cytometry. Numbers represent the percentage of CD4 T cells. (**B**–**D**) Foxp3.GFP-KI mice were immunized with MOG/CFA for the development of EAE. At the peak of disease, infiltrating cells were isolated from the CNS and Foxp3.GFP⁻CD11b⁻CD4⁺PDPN⁺ and Foxp3.GFP⁻CD11b⁻CD4⁺PDPN⁻ T cells were isolated by FACS sorting. (**B**) mRNA gene expression profiles were generated from both populations using NanoString technology. Graphs show selected genes that were consistently downregulated or upregulated in PDPN⁺ T effectors compared with PDPN⁻ T effectors in 3 independent experiments. (**C**) mRNA was isolated from both populations, and the expression patterns of *Il7ra* and *Bcl2* were confirmed by quantitative PCR. Graphs shown are representative of 2 independent experiments. (**D**) PDPN⁺ and PDPN⁻ T effector cells isolated from the CNS were analyzed for expression of PD-1 and TIM-3 by flow cytometry, and the percentage of TIM-3⁺PD-1⁺ T cells among each group is shown. (**E**) WT CD4 T cells were stimulated with plate-bound anti-CD3 and anti-CD28 Abs and differentiated in the presence of no cytokine (Th0), IL-6 and TGF-β, or IL-1β, IL-6, and IL-23. After 4 days, cultures were analyzed for expression of PDPN by flow cytometry. Data are representative of more than 3 independent experiments.

these data show that CD4 T cell–specific deletion of PDPN results in increased accumulation of CD4 T cells in the CNS and consequently leads to a more rapid onset and increased severity of EAE.

Natural PDPN⁺ T effector cells exhibit an inhibitory phenotype. We have shown that EAE overexpression of PDPN on T cells leads to reduced numbers of T effector cells in the CNS, resulting in accelerated recovery and protection of the tissue, while T cell–specific deletion of PDPN leads to an exacerbated disease course characterized by increased numbers of T effector cells in the CNS. To explore whether natural PDPN expression on T cells has similar effects on T effector cell survival, we first analyzed the kinetics of PDPN expression on T cells during the development of an immune response. During the T cell activation/priming phase following immunization of WT mice, there was no significant expression of PDPN on T cells from either the lymph nodes or spleens (Figure 6A). Consistent with our previous findings (5), effector T cells isolated from the CNS during onset and early peak of EAE were largely PDPN positive. In contrast, the frequency of PDPN⁺ T effector cells isolated from the CNS during the recovery phase of EAE was reduced (Figure 6A), suggesting that PDPN⁺ T effector cells either disappear or downregulate PDPN during the recovery phase.

In order to determine whether naturally occurring PDPN⁺ CD4 T cells show features similar to *Pdpn*TG T cells, we next compared gene expression profiles of PDPN⁺ and PDPN⁻ effector CD4 T cells. Since naturally occurring PDPN⁺ CD4 T cells are primarily found in inflamed tissues, we immunized Foxp3.GFP reporter mice to induce development of EAE, isolated PDPN⁺ and PDPN⁻FOXP3⁻ effector CD4 T cells from the CNS, and compared their gene expression profile with the multiplex NanoString nCounter technology using a custom-made code set of 199 genes. We were thus able to identify a set of genes that was consistently downregulated or upregulated in PDPN⁺ effector CD4 T cells in the CNS compared with PDPN⁻ effector CD4 T cells in the CNS (Figure 6B and Supplemental Table 2). Interestingly, we found several factors associated with T cell inhibition to be upregulated in PDPN⁺ effector CD4 T cells, such as GRAIL, TIM-3, LAG3, PD-1, and CD39. Moreover, several prosurvival factors, including BCL2, FOXO1, and IL-7Rα, were downregulated in PDPN⁺ effector CD4 T cells in the CNS. These data indicate that PDPN⁺ T cells may be readily inhibited and more susceptible to apoptosis.

To validate the downregulation of prosurvival factors in PDPN⁺ CD4 T cells, we measured mRNA levels of *Bcl2* and *Il7ra* in PDPN⁺ and PDPN⁻ effector CD4 T cells isolated from the CNS

at the peak of disease by quantitative PCR (Figure 6C). Analogous to our NanoString analysis, both BCL2 and IL-7Rα were reduced in natural PDPN$^+$ effector CD4 T cells. Furthermore, we analyzed natural PDPN$^+$ and PDPN$^-$ effector CD4 T cells isolated from the CNS at the peak of disease for expression of the inhibitory molecules TIM-3 and PD-1 on the cell surface. Consistent with the NanoString data, the frequency of TIM-3$^+$PD-1$^+$ double-positive cells was significantly increased in PDPN$^+$ effector CD4 T cells compared with PDPN$^-$ effector CD4 T cells (Figure 6D).

Overall, these data show that natural PDPN$^+$ effector CD4 T cells in inflamed tissues preferentially coexpress other inhibitory receptors and downregulate prosurvival factors including IL-7Rα, indicating that naturally occurring PDPN$^+$ T effector cells have similar features as *Pdpn*TG T effector cells, may be more easily regulated and relatively short-lived, and thereby limit tissue inflammation.

We and others have described previously that Th17 cells come in different flavors (17). Thus, Th17 cells generated in the presence of IL-6 and TGF-β (without IL-23) are not pathogenic and fail to induce EAE upon adoptive transfer. On the other hand, Th17 cells generated in the presence of IL-1β, IL-6, and IL-23 are highly pathogenic and cause severe tissue inflammation upon adoptive transfer. Given that PDPN may serve to limit long-term survival and/or effector functions of T cells in the target organ, we hypothesized that Th17 cells may express PDPN to curb their own pathogenicity. To test this hypothesis, we determined expression of PDPN on Th17 cells generated by IL-6 and TGF-β compared with those generated by IL-1β, IL-6, and IL-23. Intriguingly, we found high PDPN expression on "nonpathogenic" Th17 cells, whereas "pathogenic" Th17 cells expressed only very little PDPN (Figure 6E). Since PDPN is coexpressed with other inhibitory cell surface receptors (TIM-3, PD-1) on T cells in the CNS, our studies suggest that PDPN is used to limit survival and quench pathogenicity of autoreactive effector T cells and thus inhibit autoimmunity.

Discussion

The data presented here indicate that expression of PDPN on T cells may limit the persistence of aggressive T effector cells in the target organ. Thus, we have shown that lack of PDPN leads to exaggerated T cell responses, as suggested by inflammatory infiltrates in multiple organs in globally PDPN-deficient mice, development of spontaneous EAE in PDPN-deficient mice on the 2D2 background, and exacerbated EAE with increased accumulation of CD4 effector T cells in the CNS of T cell–specific *Pdpn*KO mice (Figure 1, Table 1, and Figure 5). In contrast, *Pdpn*TG mice showed severe peripheral lymphopenia and a reduced number of effector T cells in the CNS during EAE, resulting in accelerated recovery (Figures 2 and 4). These data are similar to many observations made with other T cell inhibitory receptors (reviewed in ref. 2). For example, CTLA-4–deficient mice develop multiorgan autoimmunity (10), TIGIT-deficient mice crossed to the 2D2 background develop spontaneous EAE (18), and TIM-3 transgenic mice have hypoproliferative T cells and develop attenuated EAE (19). These parallels indicate that PDPN may also play a role in inhibiting T cell responses.

We describe here that both, in *Pdpn*TG T cells and in naturally occurring PDPN$^+$ T cells in the CNS, expression of PDPN and IL-7Rα are inversely correlated, suggesting that PDPN may inhibit T cell responses by reducing responsiveness to IL-7 survival signals. On the one hand, IL-7 survival signals are essential for normal T cell homeostasis in naive mice. This explains why *Pdpn*TG high expressors display severe peripheral lymphopenia, in which loss of naive T cells (which had the highest expression of PDPN on their surface) was more pronounced than loss of memory and Treg populations (Supplemental Figure 6).

On the other hand, IL-7 signals are not crucial during the T cell activation/acute phases of an immune response, but after acute activation signals fade, T cells recover IL-7Rα expression and rely on IL-7 signals once again for long-term maintenance of T effector cells. Consistent with our hypothesis that the inhibitory effects of PDPN are most evident in situations in which T cells require IL-7 signals, our data suggest that, unlike CTLA-4, PD-1, or TIGIT, PDPN does not seem to directly interfere with TCR signaling or dampen T cell activation. This is supported by our observation that *Pdpn*TG and WT mice have a similar EAE disease course during the initial phase in terms of disease incidence, onset, and maximum score (Figure 4) and by the fact that in vitro–generated Th17 cells have a very activated phenotype despite high levels of PDPN on their surface. In contrast, during active EAE, CTLA-4 T cell transgenic mice show reduced maximum disease severity (20), and many studies have shown that CTLA-4 and PD-1 directly inhibit T cell activation (2). The molecular basis for this difference most likely lies in the fact that PDPN does not have an immunoreceptor tyrosine-based inhibitory motif (ITIM) in its short cytoplasmic tail, which is required for CTLA-4, PD-1, and TIGIT to modulate TCR signaling (2). The inhibitory effects of PDPN become more apparent and important in the later phases of disease, as indicated by the more rapid recovery associated with a reduced number of T effector cells in the CNS of *Pdpn*TG mice (Figure 4), the increased number of T effector cells in the CNS of T cell–specific *Pdpn*KO mice (Figure 5), and the disappearance of natural PDPN$^+$ T effector cells in the CNS after the peak of disease (Figure 6A). Thus, PDPN may promote tissue tolerance by interfering with T effector cell survival and maintenance rather than initial activation or differentiation.

Aside from the inhibitory effects of PDPN expression on T cells, we have described previously that global PDPN expression also supports the formation of eLFs in the CNS induced by adoptive transfer of Th17 cells (5, 21). Therefore, the important question that arises is how PDPN can inhibit T cell function and also promote ectopic follicle formation. One possibility is that ectopic follicle formation requires expression of PDPN primarily on stromal cells and/or APCs rather than on T cells. Another possibility is that these two divergent effector functions of PDPN may depend on different ligands that PDPN$^+$ T cells interact with during an immune reaction. Thus, one could hypothesize that interaction with one ligand mediates T cell inhibition, while interaction with another ligand promotes eLF formation. Here, it is important to note that we predominantly observed eLF formation only after adoptive transfer of Th17 cells, but not in active EAE in which a mixture of Th1 and Th17 cells is present in the CNS. Thus, pure Th17 cells seem to create a special tissue microenvironment conducive to eLF formation, and, consequently, different ligands may be expressed in "Th17-adoptive-transfer-EAE" compared with "active EAE." PDPN has 3 known ligands: CLEC-2 (22), galectin-8 (23), and the chemokine CCL21 (24). Expression of CLEC-2 is largely restricted to hematopoietic cells, including platelets, DCs (25), and B cells (26). We

have shown here that the T cell lymphopenia and reduction in IL-7Rα levels seen in *Pdpn*TG mice is dependent upon CLEC-2 (Supplemental Figure 7). Based on this information, it is tempting to speculate that the interaction of PDPN$^+$ T cells with CLEC-2$^+$ cells might lead to T cell inhibition. However, we cannot exclude the possibility that galectin-8, a tandem-repeat type lectin, which is ubiquitously expressed by both hematopoietic and nonhematopoietic cells, may also play a role in PDPN-mediated T cell inhibition, particularly since several other galectin family members have been associated with T cell inhibition (23, 27). Finally, the chemokine CCL21 is critical for organizing lymph node structure and potentially also ectopic lymphoid structures, as it guides dendritic cells and lymphocytes toward the T cell zone (28). Thus, it is possible that, in an acute inflammatory setting, PDPN$^+$ CD4 effector T cells will be eliminated quickly due to binding to the inhibitory ligand, whereas in chronic inflammatory scenarios, PDPN$^+$ T cells may bind CCL21, thereby avoiding the inhibitory interaction, promoting formation of ectopic follicles, and propagating chronic inflammation. In this context, it is interesting to note that formation of eLFs typically occurs in chronic diseases, including autoimmune diseases like MS, rheumatoid arthritis, and myasthenia gravis, and chronic infections, for example, with *Borrelia burgdorferi*, but not in acute infections that resolve quickly (29). Importantly, these seemingly contradictory effects and functions of PDPN are reminiscent of another inhibitory T cell receptor, PD-1: although PD-1 strongly inhibits T cell responses and promotes tissue tolerance (reviewed in ref. 30), it is also expressed on follicular T helper cells in the lymph nodes and promotes germinal center reactions (31).

Although PDPN is specifically expressed on Th17 cells in vitro, during EAE we detected PDPN expression on both IL-17$^+$ and IL-17$^-$ T cells in the CNS. However, considering that cell fate mapping studies in IL-17A^{Cre} mice showed that the vast majority of CNS-infiltrating T cells are Th17 or "ex-Th17" cells, producing either IL-17 or IFN-γ or both (32), it is possible that even PDPN$^+$IL-17$^-$IFN-γ$^+$ T cells in the CNS are actually "ex-Th17" cells. Even though PDPN may not be exclusively expressed on Th17 cells in vivo, we speculate that expression of PDPN serves to primarily shut off Th17 responses. As highly proinflammatory T cells, Th17 cells have the potential to cause irreversible tissue damage and therefore need to be tightly regulated. Intriguingly, a recent report showed that expression of IL-7Rα is essential for maintenance and expansion of Th17 responses during EAE (33). In addition, IL-7Rα expression is increased on highly pathogenic Th17 cells (34), whereas PDPN is more highly expressed on "nonpathogenic" Th17 cells in vitro (Figure 6E), supporting the hypothesis that Th17 cells may express PDPN to curb their own pathogenicity.

In conclusion, the data presented here show that expression of PDPN on T cells can limit survival and accumulation of T effector cells in the target tissue. We propose that, after acute inflammation, PDPN on T cells serves primarily to control long-term Th17 responses in the target organ by reducing sensitivity to IL-7 survival signals, thereby preventing tissue damage.

Methods

Mice. C57BL/6, Ly5.1, and *Cd4-Cre* mice were obtained from The Jackson Laboratory. 2D2 mice (12) and Foxp3.GFP-KI mice (35) have been described previously. *Pdpn*$^{-/-}$ mice on 129Sv background (8) were provided by Maria Ramirez (Boston University, Boston, Massachusetts, USA) and crossed with C57BL/6 and 2D2 mice in house. For the generation of *Pdpn*TG mice, the cDNA of PDPN (C57BL/6 strain) was cloned into the human CD2 expression cassette (Supplemental Figure 2 and ref. 36). The construct was microinjected directly into C57BL/6 oocytes, yielding 3 independent founders: line 552, line 556, and line 560. *Pdpn*$^{fl/fl}$ mice were generated at Taconic Artemis by insertion of loxP sites flanking exon 3 of the PDPN allele using standard methods and backcrossed to C57BL/6J mice for more than 6 generations at the University of Birmingham and then bred in house. *Pdpn*$^{fl/fl}$ mice were crossed with *Cd4-Cre* mice and 2D2 mice in house. *Clec2*$^{-/-}$ mice on 129Sv background were provided by Shannon Turley (Dana-Farber Cancer Institute, Boston, Massachusetts, USA) and crossed with *Pdpn*TG mice (line 560) in house. All mice were housed in a specific pathogen–free viral antibody-free animal facility at the Harvard Institutes of Medicine.

Induction and assessment of EAE. *Pdpn*TG mice (552), WT mice, *Pdpn*$^{fl/fl}$ *Cd4-Cre* mice, *Pdpn*$^{fl/fl}$ mice, and Foxp3.GFP KI mice were injected s.c. with 100 μg $MOG_{35–55}$ peptide emulsified in CFA (Difco), which was supplemented with 4 mg/ml *Mycobacterium tuberculosis* H37 RA (Difco). Mice also received 100 ng pertussis toxin (List Biological Laboratories Inc.) i.v. on days 0 and 2 after immunization. Animals were monitored daily for the development of signs of EAE according to the following criteria: 0, no disease; 1, decreased tail tone or mild balance defects; 2, hind limb weakness, partial paralysis, or severe balance defects that cause spontaneous falling over; 3, complete hind limb paralysis or very severe balance defects that prevent walking; 4, front and hind limb paralysis or inability to move body weight into a different position; 5, moribund state.

Isolation of cells from the CNS. WT, *Pdpn*TG, and Foxp3.GFP KI mice were sacrificed at the peak of disease and perfused through the left cardiac ventricle with PBS. Brains and spinal cords were cut into pieces and digested for 30 minutes at 37°C with Collagenase D (Roche) at a concentration of 2.5 mg/ml and Deoxyribonuclease I (Sigma-Aldrich) at a concentration of 1 mg/ml. To prepare a single cell suspension, the tissues were mashed and passed through a 70-μm mesh. Mononuclear cells were isolated over a 37%/70% Percoll gradient (GE healthcare). Cells were either directly analyzed for expression of surface molecules by flow cytometry or cells were stimulated for 3 hours with 50 ng/ml phorbol 12-myristate 13-acetate (Sigma-Aldrich) and 1 μM ionomycin (Sigma-Aldrich) in the presence of monensin (GolgiStop, BD Pharmingen). Cells were then fixed with 0.4% paraformaldehyde (Electron Microscopy Sciences) and permeabilized with PBS containing 2% FCS and 0.1% Saponin (Sigma-Aldrich). Cells were analyzed for the production of cytokines by staining with anticytokine antibodies and subsequent flow cytometry.

Antibodies and flow cytometry. The following antibodies were used for flow cytometry: αCD4 (RM4-5), αCD8 (53-6.7), αCD25 (PC61), αCD62L (MEL-14), αCD44 (IM7), αCD11b (M1/70), αCD11c (N418), αCD19 (6D5), αNK1.1 (PK136), αCD45.1 (A20), αCD45.2 (104), αCD90.1 (OX-7), αCD90.2 (30-H12), αIFN-γ (XMG1.2), αIL-17A (TC11-18H10.1), αIL-10 (JES5-10E3), αTIM-3 (8B.2C12), αPD1 (RMPI-30), αIL-7Rα (A7R34), αPDPN (8.1.1), isotype control Syrian hamster IgG (SHG-1), rat IgG2a isotype control (RTK2758), mouse IgG1 isotype control (MOPC-21), and αVβ11 (KT11) were all purchased from BioLegend. αFOXP3 (FJK-16s) and α-γδ-TCR (eBioGL3) were purchased from eBioscience. αCD3 (1452C11) and 7AAD were purchased from BD Pharmingen. All flow cytometry data were acquired on a BD FACSCalibur or BD LSRII and analyzed with FlowJo Tree Star software.

Histopathologic analysis. Lung, liver, small and large intestine, CNS, and heart tissues were harvested from *Pdpn*$^{-/-}$ mice and their WT or heterozygous littermates. Tissues were fixed in 10% neutral buffered formalin and processed routinely for paraffin embedment. Slides were stained with hematoxylin and eosin stains. For identification of T cells by immunohistochemistry, standard avidin-biotin staining was performed on the sections with rabbit anti-mouse CD3g (Abcam), using reagents from Vector Laboratories. Normal mouse spleen tissue served as positive staining controls; negative controls included omission of the primary antibody. To quantify infiltrates in the small intestine, 2 different sections of eight to nine 1-cm pieces of small intestine were evaluated for each mouse for presence and number of small (10–20 small, round, dark-blue cells in diameter), medium (20–40 cells in diameter), and large (>40 cells in diameter) infiltrates.

For analysis of CNS inflammation in EAE, mice were sacrificed 30 days after immunization or in case of spontaneous disease after animals reached a stable score. Brains and spinal cords from 2D2 *Pdpn*$^{-/-}$ mice and 2D2 *Pdpn*$^{+/-}$ littermates and from *Pdpn*TG mice (line 552) and their WT littermates were fixed in 10% neutral buffered formalin and processed routinely for paraffin embedment. Slides were stained with Luxol fast blue-hematoxylin and eosin stains. Inflammatory foci (>10 mononuclear cells) were counted in leptomeninges and parenchyma in a blinded fashion in that the pathologist was unaware of the clinical status and genotype of the mice.

NanoString gene expression analysis. Foxp3.GFP-KI mice were immunized with MOG/CFA for the development of EAE. At the peak of disease, infiltrating cells were isolated from the CNS and Foxp3.GFP$^-$CD11b$^-$CD4$^+$PDPN$^+$ and Foxp3.GFP$^-$CD11b$^-$CD4$^+$PDPN$^-$ T effector cells were isolated by FACS sorting. Cells were then immediately lysed using RLT buffer (Qiagen). Cell lysates were hybridized with a custom-made CodeSet according to the manufacturer's instructions. Barcodes were counted (1,150 fields of view per sample) on an nCounter Digital Analyzer following the manufacturer's protocol (NanoString Technologies Inc.). Data were processed using nSolver Analysis Software first by normalization with respect to the geometric mean of the positive control spike counts (provided by manufacturer) and then with 4 reference genes (*Actb*, *Gapdh*, *Hprt*, and *Tubb5*). A background correction was done by subtracting the mean + 2 standard deviations of 8 negative control counts (provided by manufacturer) and eliminating data that were <1.

RNA isolation and quantitative PCR. RNA was extracted from sorted cells using the RNeasy Kit (Qiagen) according to the manufacturer's instructions. RNA was then transcribed into cDNA using the iScript cDNA Synthesis Kit (Bio-Rad) according to the manufacturer's instructions. Quantitative PCR primers and probes were purchased from Applied Biosystems (BCL2: Mm00477631_m1, IL-7R: Mm00434295_m1, PDPN: Mm00494716_m1, TIM-3: Mm00454540_m1, PD-1: Mm01285676_m1, β-Actin: 4352341E).

Statistics. All values are expressed as the average ± SEM. Data sets were analyzed with the aid of GraphPad Prism Software, version 6 (GraphPad). Differences between groups were assessed with either 2-tailed Student's *t* tests or, in the case of multiple groups, 1-way ANOVA with Tukey's multiple comparison test. *P* values of less than 0.05 were considered to be significant. Linear regression analysis of EAE data was performed using GraphPad Prism Software.

Study approval. Breeding and experiments were reviewed and approved by the Institutional Animal Care and Use Committee of Harvard Medical School.

Acknowledgments

We thank D. Kozoriz for cell sorting and K.D. Fowler for help with the analysis of the NanoString datasets. This work was supported by grants from the NIH (2T32HL007633-26 to P.R. Burkett, 5R01 NS059996 to E. Bettelli, and P01 AI045757, P01 AI073748, R01 NS045937, P01 AI039671, and P01 AI056299 to V.K. Kuchroo). A. Peters was supported by the German Multiple Sclerosis Society (DMSG).

Address correspondence to: Estelle Bettelli, Benaroya Research Institute, 1201 9th Ave., Seattle, Washington, USA. Phone: 206.287.1022; E-mail: ebettelli@benaroyaresearch.org. Or to: Vijay K. Kuchroo, Evergrande Center for Immunologic Diseases, Harvard Medical School and Brigham and Women's Hospital, 77 Avenue Louis Pasteur, HIM 785, Boston, Massachusetts 02115, USA. Phone: 617.525.5537; Email: vkuchroo@Evergrande.hms.harvard.edu.

1. Korn T, Bettelli E, Oukka M, Kuchroo VK. IL-17 and Th17 cells. *Annu Rev Immunol*. 2009;27:485–517.
2. Joller N, Peters A, Anderson AC, Kuchroo VK. Immune checkpoints in central nervous system autoimmunity. *Immunol Rev*. 2012;248(1):122–139.
3. Pardoll DM. The blockade of immune checkpoints in cancer immunotherapy. *Nat Rev Cancer*. 2012;12(4):252–264.
4. Sakuishi K, Apetoh L, Sullivan JM, Blazar BR, Kuchroo VK, Anderson AC. Targeting Tim-3 and PD-1 pathways to reverse T cell exhaustion and restore anti-tumor immunity. *J Exp Med*. 2010;207(10):2187–2194.
5. Peters A, et al. Th17 cells induce ectopic lymphoid follicles in central nervous system tissue inflammation. *Immunity*. 2011;35(6):986–996.
6. Schacht V, Dadras SS, Johnson LA, Jackson DG, Hong YK, Detmar M. Up-regulation of the lymphatic marker podoplanin, a mucin-type transmembrane glycoprotein, in human squamous cell carcinomas and germ cell tumors. *Am J Pathol*. 2005;166(3):913–921.
7. Astarita JL, Acton SE, Turley SJ. Podoplanin: emerging functions in development, the immune system, and cancer. *Front Immunol*. 2012;3:283.
8. Ramirez MI, Millien G, Hinds A, Cao Y, Seldin DC, Williams MC. T1alpha, a lung type I cell differentiation gene, is required for normal lung cell proliferation and alveolus formation at birth. *Dev Biol*. 2003;256(1):61–72.
9. Schacht V, et al. T1α/podoplanin deficiency disrupts normal lymphatic vasculature formation and causes lymphedema. *EMBO J*. 2003;22(14):3546–3556.
10. Waterhouse P, et al. Lymphoproliferative disorders with early lethality in mice deficient in Ctla-4. *Science*. 1995;270(5238):985–988.
11. Nishimura H, Minato N, Nakano T, Honjo T. Immunological studies on PD-1 deficient mice: implication of PD-1 as a negative regulator for B cell responses. *Int Immunol*. 1998;10(10):1563–1572.
12. Bettelli E, Pagany M, Weiner HL, Linington C, Sobel RA, Kuchroo VK. Myelin oligodendrocyte glycoprotein-specific T cell receptor transgenic mice develop spontaneous autoimmune optic neuritis. *J Exp Med*. 2003;197(9):1073–1081.
13. Ma A, Koka R, Burkett P. Diverse functions of IL-2, IL-15, and IL-7 in lymphoid homeostasis. *Annu Rev Immunol*. 2006;24:657–679.
14. Li J, Huston G, Swain SL. IL-7 promotes the transition of CD4 effectors to persistent memory cells. *J Exp Med*. 2003;198(12):1807–1815.
15. Christou CM, et al. Renal cells activate the platelet receptor CLEC-2 through podoplanin. *Biochem J*. 2008;411(1):133–140.
16. Suzuki-Inoue K, et al. Essential in vivo roles of the C-type lectin receptor CLEC-2: embryonic/neonatal lethality of CLEC-2-deficient mice by blood/lymphatic misconnections and impaired thrombus formation of CLEC-2-deficient platelets.

J Biol Chem. 2010;285(32):24494–24507.
17. Peters A, Lee Y, Kuchroo VK. The many faces of Th17 cells. *Curr Opin Immunol*. 2011;23(6):702–706.
18. Joller N, et al. Cutting edge: TIGIT has T cell-intrinsic inhibitory functions. *J Immunol*. 2011;186(3):1338–1342.
19. Dardalhon V, et al. Tim-3/galectin-9 pathway: regulation of Th1 immunity through promotion of $CD11b^+Ly^-6G^+$ myeloid cells. *J Immunol*. 2010;185(3):1383–1392.
20. Engelhardt JJ, Sullivan TJ, Allison JP. CTLA-4 overexpression inhibits T cell responses through a $CD28^-$B7-dependent mechanism. *J Immunol*. 2006;177(2):1052–1061.
21. Jäger A, Dardalhon V, Sobel RA, Bettelli E, Kuchroo VK. Th1, Th17, and Th9 effector cells induce experimental autoimmune encephalomyelitis with different pathological phenotypes. *J Immunol*. 2009;183(11):7169–7177.
22. Suzuki-Inoue K, et al. Involvement of the snake toxin receptor CLEC-2, in podoplanin-mediated platelet activation, by cancer cells. *J Biol Chem*. 2007;282(36):25993–26001.
23. Cueni LN, Detmar M. Galectin-8 interacts with podoplanin and modulates lymphatic endothelial cell functions. *Exp Cell Res*. 2009;315(10):1715–1723.
24. Kerjaschki D, et al. Lymphatic neoangiogenesis in human kidney transplants is associated with immunologically active lymphocytic infiltrates. *J Am Soc Nephrol*. 2004;15(3):603–612.
25. Colonna M, Samaridis J, Angman L. Molecular characterization of two novel C-type lectin-like receptors, one of which is selectively expressed in human dendritic cells. *Eur J Immunol*. 2000;30(2):697–704.
26. Mourao-Sa D, et al. CLEC-2 signaling via Syk in myeloid cells can regulate inflammatory responses. *Eur J Immunol*. 2011;41(10):3040–3053.
27. Liu FT, Rabinovich GA. Galectins: regulators of acute and chronic inflammation. *Ann N Y Acad Sci*. 2010;1183:158–182.
28. Turley SJ, Fletcher AL, Elpek KG. The stromal and haematopoietic antigen-presenting cells that reside in secondary lymphoid organs. *Nat Rev Immunol*. 2010;10(12):813–825.
29. Weyand CM, Kurtin PJ, Goronzy JJ. Ectopic lymphoid organogenesis: a fast track for autoimmunity. *Am J Pathol*. 2001;159(3):787–793.
30. Francisco LM, Sage PT, Sharpe AH. The PD-1 pathway in tolerance and autoimmunity. *Immunol Rev*. 2010;236:219–242.
31. Good-Jacobson KL, Szumilas CG, Chen L, Sharpe AH, Tomayko MM, Shlomchik MJ. PD-1 regulates germinal center B cell survival and the formation and affinity of long-lived plasma cells. *Nat Immunol*. 2010;11(6):535–542.
32. Hirota K, et al. Fate mapping of IL-17-producing T cells in inflammatory responses. *Nat Immunol*. 2011;12(3):255–263.
33. Liu X, et al. Crucial role of interleukin-7 in T helper type 17 survival and expansion in autoimmune disease. *Nat Med*. 2010;16(2):191–197.
34. Lee Y, et al. Induction and molecular signature of pathogenic TH17 cells. *Nat Immunol*. 2012;13(10):991–999.
35. Bettelli E, et al. Reciprocal developmental pathways for the generation of pathogenic effector TH17 and regulatory T cells. *Nature*. 2006;441(7090):235–238.
36. Lang G, et al. The structure of the human CD2 gene and its expression in transgenic mice. *EMBO J*. 1988;7(6):1675–1682.